

# SUPER-RESOLUTION RESULTS FOR A 1D INVERSE SCATTERING PROBLEM

Wenjie Wang, Yue Li, Zhao Li, Ross Murch

Department of Electronic and Computer Engineering  
Hong Kong University of Science and Technology, Hong Kong, China.

Email: [wwangbk@connect.ust.hk](mailto:wwangbk@connect.ust.hk), [ylidu@connect.ust.hk](mailto:ylidu@connect.ust.hk), [eelizhao@ust.hk](mailto:eelizhao@ust.hk),  
[eermurch@ust.hk](mailto:eermurch@ust.hk)

## ABSTRACT

In this work we consider the one-dimensional (1D) inverse scattering problem of super-resolving the location of discrete point scatters satisfying the 1D Helmholtz equation. This inverse problem has important applications in the detection of shunt faults in electrical transmission lines and leaks in water pipelines where usually only low frequency spectral information is available from measurements. We formulate the inverse scattering problem as a sparse reconstruction problem and apply convex optimization to super-resolve the location of point scatters. We extend previous results and prove that we can super-resolve up to 4 points and 5-18 points with infinite precision if the points are separated by  $1/(2f_c)$  and  $1/f_c$  respectively ( $f_c$  is the maximum frequency we can measure). This is over 4 times closer than previous results. Simulation results are used to demonstrate the effectiveness of the approach.

**Index Terms**— Inverse scattering, super-resolution, restricted isometry property, transmission lines

## 1. INTRODUCTION

Super-resolution is an important technique used in imaging, and more generally inverse scattering, where limited resolution measurement data is utilized to extract high resolution details about an image or object [1–6]. Its use has been most popular in the image processing arena and applied to applications such as astronomical imaging. However, important one-dimensional (1D) applications where super-resolution can be applied are also appearing. For example detecting faults in electrical cables and water pipelines has recently attracted attention [7–14]. This is due to the electrification of infrastructure which has led to extensive networks of cables, optical fibers and transmission lines in cars, ships, airplanes and buildings. Analogously fault or leak detection for pipelines carrying water, oil and gas also has important safety and financial implications (e.g. urban water supply systems world wide lose approximately 30% of their water from leakage [15]). Locating cable faults, potential cable faults, pipeline leaks and potential leaks is therefore important. Both

problems can be formulated using a common "imaging" or inverse scattering framework based on the 1D Helmholtz equation [12–14]. While methods for this 1D inverse scattering problem have existed for sometime their application to specific engineering problems using super-resolution has been limited and further research is required to apply them. Compared with alternative high resolution methods (e.g. MUSIC or ESPRIT like methods), our inverse scattering problem with super-resolution only requires a single sensor instead of measurements from multiple sensors [16].

Our interest in applying super-resolution to 1D inverse scattering systems is that the spectral measurements obtained from them are often limited to low frequencies. In the case of water pipelines this is because the models we use are only satisfied at low frequencies and therefore we need to restrict our measurements to those frequencies. In the case of electrical cables it is because attenuation on the line at high frequencies becomes large and signals cannot be measured.

Super-resolution is broadly defined as the problem of recovering fine details of an object from low frequency spectral measurements of scattering parameters [5]. A mathematical theory of super-resolution was proposed in 2014 [2] and a key result was that if Fourier samples could be obtained up to frequencies  $f_c$  then the location of discrete points in 1D could be precisely obtained if the points were separated by at least  $2/f_c$ . Related work for 1D applications includes compressive sensing [3, 6, 17] in which the problem of recovering a signal with partial data is considered. In compressive sensing, the partial data is the observation which is uniformly distributed across the complete spectrum while in super-resolution we only have access to the lower end of the complete spectrum. Therefore, restrictions are needed on the separation of points in the object to ensure that super-resolution is feasible.

Our contribution is to show that for a particular number  $s$  of discrete scatters or faults then they can be perfectly reconstruction if they are separated by at least  $1/(2f_c)$  for  $s \leq 4$  and by at least  $1/f_c$  for  $5 \leq s \leq 18$ . For  $s > 18$  the separation criteria reverts back to the previous larger bound  $2/f_c$ . We formulate the inverse scattering problem as a sparse reconstruction problem and apply convex optimization to super-resolve the faults. We demonstrate the effectiveness of the ap-

We would like to thank the Hong Kong Research Grants Council for the General Research Fund Grant 16232316.

proach with simulation results for faults along a transmission line.

In section 2 we introduce the inverse scattering problem and find expressions for the discrete faults in terms of reflectivity. In section 3, the super-resolution scheme is presented and the proof of conditional well-posedness of the super-resolution technique is given. In section 4 we provide simulation results to verify the effectiveness and validity of the approach.

## 2. PROBLEM FORMULATION

We consider the 1D inverse scattering problem of reconstructing discrete point scatters or faults from scattering measurements satisfying the 1D Helmholtz equation. A particular example is shown in Fig. 1 for transmission lines where a point scatter or fault  $\Delta G(x)$  is shown in addition to the conventional transmission line parameters of inductance  $L$  and capacitance  $C$ . The value of  $\Delta G(x)$  denotes the size of the shunt conductance fault. Frequency  $f$  of the scattering is related to propagation speed  $c$  and wavenumber  $k$  through  $f = kc/2\pi$ . The inverse scattering problem can then be defined as reconstructing the size and position of the discrete faults  $\Delta G(x)$  from measurements of the scattered voltages  $V_s(x, k)$  at position  $x = 0$  due to an incident source voltage  $V_{inc}(x, k)$  also at  $x = 0$ .

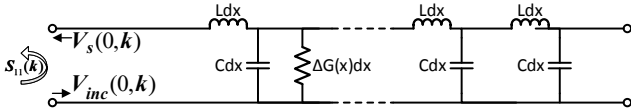


**Fig. 1.** Distributed transmission line model for an infinitesimal section of length  $dx$  in which one discrete fault  $\Delta G(x)$  is shown.

More generally the inverse problem also models a water pipeline where voltages are replaced by acoustic pressures and shunt faults are related to leak sizes [14]. Writing the inverse scattering measurements in terms of reflectivity  $S_{11}$ , which is defined as,

$$S_{11}(k) = \frac{V_s(0, k)}{V_{inc}(0, k)} \quad (1)$$

we find that the faults  $\Delta G(x)$  are related to measurements through a Fourier Transform [13]. In particular the relation can be written as

$$S_{11}(k) = -\frac{1}{2} \int_0^{\mathcal{L}} \Delta G(y) Z_0 \cdot e^{-2jk_y} dy. \quad (2)$$

where  $\mathcal{L}$  is the total length of the transmission line or pipeline and  $Z_0$  is known as the characteristic impedance of the line ( $Z_0 = \sqrt{L/C}$  for transmission lines). While the result in Eq. (2) is based on the Born approximation it has been shown to be accurate over a very wide range of fault sizes [12–14]. In order to reconstruct  $\Delta G(x)$  along the line we apply the

inverse Fourier transform to Eq. (2) and arrive at

$$\mathcal{F}^{-1}[S_{11}(k)](2x) = -\frac{1}{2} \Delta G(x) Z_0. \quad (3)$$

An example of a reconstruction with  $s = 3$  faults using this approach is shown in Fig. 2 for a transmission line of length  $\mathcal{L} = 0.5$  m and different bandwidths  $0 \leq f \leq f_c$ . For large bandwidths  $f_c = 50$  GHz the faults are perfectly reconstructed but for lower bandwidths it can be observed the faults are smeared out or defocused.

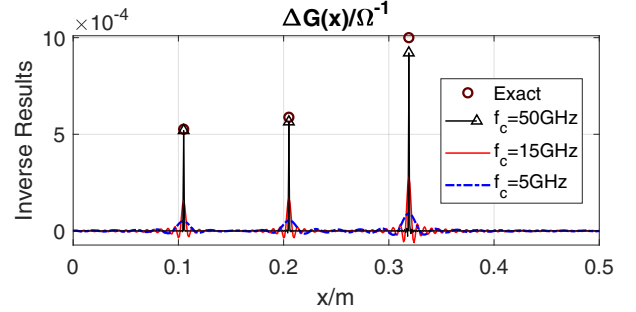


**Fig. 2.** Reconstruction results of  $\Delta G(x)$  with different  $f_c$ . The transmission line has length 0.5 m and 3 shunt faults ( $\Delta G(0.105\text{m}) = 1/1900\Omega$ ,  $\Delta G(0.205\text{m}) = 1/1700\Omega$  and  $\Delta G(0.319\text{m}) = 1/1000\Omega$ ) are included.

## 3. THE SUPER-RESOLUTION APPROACH

### 3.1. Super-Resolution Scheme

Using a continuous-time model the reflectivity, Eq. (3), can be written as a weighted superposition of spikes

$$P = \mathcal{F}^{-1}[S_{11}(f)](t) = \sum_{j=1}^s a_j \delta_{t_j}, \quad (4)$$

where  $\{t_j\}$  are fault locations in  $[0, 1]$  and  $\delta_\tau$  is a Dirac measure at  $\tau$ . We only have access to the lower end of the spectrum  $|f| \leq f_c$  in the form of the Fourier series coefficients

$$S_{11}(f) = \int_0^1 P e^{-i2\pi ft} dt, |f| \leq f_c, f \in \mathbb{Z}, \quad (5)$$

For simplicity, we shall use matrix notations [2] to relate the measurement  $S_{11}$  and the profile  $P$  and will write Eq. (5) as  $S_{11} = \mathcal{F}_B P$ , where  $\mathcal{F}_B$  is a linear map operating on the frequency range  $[-f_c, f_c]$  [2].

Our objective here is to reconstruct  $P$  exactly from the band limited measurement  $S_{11}$ . Hence, the following  $\ell_1$  minimization objective has been proposed [2]:

$$\min_{\tilde{P}} \|\tilde{P}\|_{\ell_1} \quad \text{s.t.} \quad S_{11} = \mathcal{F}_B \tilde{P}. \quad (6)$$

### 3.2. The Restricted Isometry Property

It is important to determine whether Eq. (6) is well-posed to show that a super-resolution solution exists. A particular criteria for evaluating this is by using the Restricted Isometry Property (RIP), proposed in [17] as

**Definition 1.** For each integer  $s = 1, 2, \dots$ , define the isometry constant  $\delta_s$  of a linear map  $A$  as the smallest number such that

$$(1 - \delta_s)\|x\|_{\ell_2}^2 \leq \|Ax\|_{\ell_2}^2 \leq (1 + \delta_s)\|x\|_{\ell_2}^2 \quad (7)$$

holds for such  $s$ -sparse signal  $x$ .  $x$  is said to be  $s$ -sparse if it has at most  $s$  nonzero entries.

**Remark.** A necessary and sufficient condition for well-posedness of Eq. (6) with  $s$ -sparse  $P$  requires that  $\hat{\mathcal{F}}_B$  satisfies the Restricted Isometry Property with  $\delta_{2s} < 1$ , where  $\hat{\mathcal{F}}_B$  is  $\mathcal{F}_B$  with its columns normalized [18].

For  $s$  faults we therefore require  $\delta_{2s}$  to be less than unity. Intuitively, this requires that every  $2s$  columns of  $\hat{\mathcal{F}}_B$  must be nearly orthogonal (has cross-correlation coefficient small enough to satisfy RIP). However, the cross-correlations of any two columns, i.e.  $\hat{\mathcal{F}}_{t_i}$  corresponds to  $t_i$  and  $\hat{\mathcal{F}}_{t_j}$  corresponds to  $t_j$ , in  $\hat{\mathcal{F}}_B$  can be written as

$$c(t_i, t_j) = \frac{|\langle \hat{\mathcal{F}}_{t_i}, \hat{\mathcal{F}}_{t_j} \rangle|}{\|\hat{\mathcal{F}}_{t_i}\|_{\ell_2} \|\hat{\mathcal{F}}_{t_j}\|_{\ell_2}} = \left| \frac{\sin[\pi(2f_c + 1)|t_i - t_j|]}{(2f_c + 1)\sin(\pi|t_i - t_j|)} \right|. \quad (8)$$

The cross-correlation of two consecutive columns in  $\hat{\mathcal{F}}_B$  can be seen to be close to 1. Thus, the sub-Fourier mapping  $\hat{\mathcal{F}}_B$  does not obey the restricted isometry property [2]. However, we also notice that the cross-correlation of two columns in  $\hat{\mathcal{F}}_B$  decreases if their separation increases (see Eq. (8)). It is therefore possible to reconstruct such  $s$ -sparse  $P$  if nonzero entries are sufficiently separated. To characterize this situation we define the minimum separation between faults and then prove what the minimum separation should be to ensure the well-posedness of the super-resolution algorithm under various conditions.

**Definition 2.** Let  $T = \{t_j\}$  be the support of  $P$  in Eq. (4), then the minimum separation of spikes in  $P$  is defined as

$$\Delta(T) = \min_{t, t' \in T, t \neq t'} |t - t'|_{\Delta}, \quad (9)$$

where  $|t - t'|_{\Delta}$  is the wrap-around distance, e.g. for  $t \in [0, 1]$ ,  $t = 0$  and  $t' = \frac{3}{4}$ ,  $|t - t'|_{\Delta} = \frac{1}{4}$ .

### 3.3. Conditional well-posedness

**Theorem 1.** If  $s \leq 4$ , there exists a constant  $\delta_{2s} < 1$  such that

$$(1 - \delta_{2s})\|P\|_{\ell_2}^2 \leq \|\hat{\mathcal{F}}_B P\|_{\ell_2}^2 \leq (1 + \delta_{2s})\|P\|_{\ell_2}^2 \quad (10)$$

holds for any  $2s$ -sparse signal  $P$  with its support satisfying  $\Delta(T) \geq \frac{1}{2f_c}$ .

**Theorem 2.** If  $5 \leq s \leq 18$ , there exists a constant  $\delta_{2s} < 1$  such that

$$(1 - \delta_{2s})\|P\|_{\ell_2}^2 \leq \|\hat{\mathcal{F}}_B P\|_{\ell_2}^2 \leq (1 + \delta_{2s})\|P\|_{\ell_2}^2$$

holds for any  $2s$ -sparse signal  $P$  with its support satisfying  $\Delta(T) \geq \frac{1}{f_c}$ .

The proof of Theorem. 1 and Theorem. 2 is as follows. For any  $2s$ -sparse signal  $P$  with nonzero entries labeled in ascending order as  $p_{t_i}$ ,  $i \in E_{2s} = \{1, 2, 3, \dots, 2s\}$  then

$$\frac{\|\hat{\mathcal{F}}_B P\|_{\ell_2}^2}{\|P\|_{\ell_2}^2} = 1 + \frac{\sum_{i \in E_{2s}} \sum_{j \in E_{2s} \setminus \{i\}} \langle \hat{\mathcal{F}}_{t_i}, \hat{\mathcal{F}}_{t_j} \rangle p_{t_i}^* \cdot p_{t_j}}{\sum_{i=1}^{2s} |p_{t_i}|^2}, \quad (11)$$

where  $E_{2s} \setminus \{i\}$  denotes the relative complement of  $\{i\}$  with respect to the set  $E_{2s}$  and the superscript  $*$  denotes the complex conjugate.

Given the assumption that  $\Delta(T) \geq \frac{n}{2f_c}$  ( $n \in \mathbb{N}$ ), the cross-correlations between any two columns in  $\hat{\mathcal{F}}_B$  that corresponds to nonzero entries of  $P$  can be simplified from Eq. (8) as

$$c(t_i, t_j) \simeq \left| \frac{\sin[\pi(2f_c + 1)|t_i - t_j|_{\Delta}]}{\pi(2f_c + 1)|t_i - t_j|_{\Delta}} \right| \quad (12)$$

$$\leq \frac{1}{(n|i - j|_{\Delta} + 0.5)\pi},$$

where  $|i - j|_{\Delta}$  is the the wrap-around separation. e.g. for  $E_8 = \{1, 2, 3, \dots, 8\}$ ,  $i = 1$  and  $j = 8$ ,  $|i - j|_{\Delta} = 1$ . Then, by combining Eq. (10) with Eq. (11) and noting that  $\|\hat{\mathcal{F}}_{t_i}\|_{\ell_2} = 1$  we get [18]

$$\delta_{2s} \leq \frac{\sum_{i \in E_{2s-1}} \sum_{j \in E_{2s} \setminus E_i} c(t_i, t_j) \left[ |p_{t_i}|^2 + |p_{t_j}|^2 \right]}{\sum_{i=1}^{2s} |p_{t_i}|^2} \quad (13)$$

$$= \frac{\sum_{i=1}^{2s} \left\{ \sum_{j \in E_{2s} \setminus \{i\}} c(t_i, t_j) |p_{t_j}|^2 \right\}}{\sum_{i=1}^{2s} |p_{t_i}|^2}$$

$$\leq \max_{i \in E_{2s}} \left\{ \sum_{j \in E_{2s} \setminus \{i\}} c(t_i, t_j) \right\}$$

$$\leq \sum_{d=1}^{s-1} \frac{2}{(nd + 0.5)\pi} + \frac{1}{(ns + 0.5)\pi}.$$

As a result, the upper bound of  $\delta_{2s}$  for any concrete set-up can be calculated by Eq. (13). For  $s = 2, 3, 4$ ,  $\delta_{2s} < 1$  for  $\Delta(T) \geq 1/(2f_c)$ . For  $5 \leq s \leq 18$ , it requires  $\Delta(T) \geq 1/f_c$ . This concludes the proof of Theorem. 1 and Theorem. 2.

The upper bound of  $\delta_{2s}$  with different  $\Delta(T)$  is also plotted in Fig. 3 to illustrate its properties. To begin with, it is important to bear in mind that, according to the Rayleigh limit, the minimum separation for possibly identifying two distinct faults is  $\Delta(T) > 1/(2f_c)$ . Given that  $\delta_4 < 0.6$  and  $\delta_6 < 0.8$  for  $\Delta(T) \geq 1/(2f_c)$ , it can be deduced that there

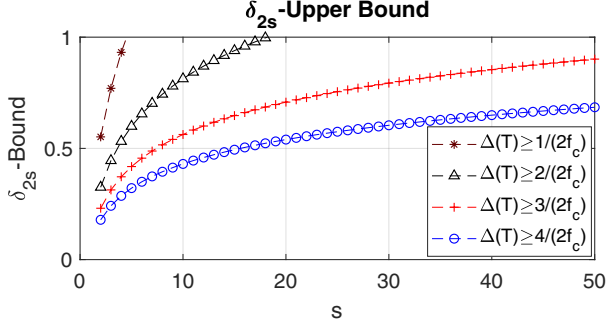


**Fig. 3.** Upper Bound of  $\delta_{2s}$  with different  $\Delta(T)$

exists a constant  $\alpha < 1$  so that the  $\delta_4 < 1$  and  $\delta_6 < 1$  for  $\Delta(T) \geq \alpha/(2f_c)$ . This indicates that our super-resolution technique can potentially reconstruct the impulse response beyond the Rayleigh criteria when there are 2 or 3 spikes. It is also important to mention that if the minimum separation  $\Delta(T) \geq 2/f_c$ , the  $\delta_{2s}$  is generally upper-bounded by 1. Thus, the reconstruction through Eq. (6) is unique for the general case as long as  $\Delta(T) \geq 2/f_c$ , which is consistent with Theorem 1.2 in [2].

#### 4. SIMULATION RESULTS

Numerical examples are provided to demonstrate the validity of our super-resolution results. A transmission line with  $N_s = \{7, 6, 5, 4\}$  shunt defects with length  $\mathcal{L} = 1$  m and  $c = 2 \times 10^8$  m/s is considered. The scattering parameter  $S_{11}(k)$  is collected up to  $f_c$  with 10 MHz frequency intervals. The minimum distance between shunt conductance defects  $d_x$  is set to 0.1 m ( $\Delta(T) = 2d_x/c = 1$  ns). For each  $N_s$  the fault profiles are generated randomly in both location ( $\Delta(T) = 1$  ns) and value ( $G \in [1/2000\Omega, 1/1000\Omega]$ ). For each setting, 10 trials are conducted.

Due to the necessary discretization of  $\mathcal{F}_B$  for simulation, a relaxed version of Eq. (6) is used in which

$$\min_{\tilde{P}} \frac{1}{2} \|S_{11} - \mathcal{F}_B \tilde{P}\|_{\ell_2}^2 + \tau \|\tilde{P}\|_{\ell_1}. \quad (14)$$

To solve problem (14) we used CVX, a package for specifying and solving convex programs [19, 20].

To demonstrate the effect of noise on the performance of the super-resolution technique, we set  $N_s = 5$  and add complex white Gaussian noise  $N(k)$  to the  $S_{11}(k)$  with different SNR defined as

$$\text{SNR} = 20 \log_{10} \left[ \frac{\|S_{11}\|_{\ell_2}}{\|N\|_{\ell_2}} \right]. \quad (15)$$

For each SNR level, 30 trials are conducted.

In order to calculate the reconstruction error in the approaches we first integrate the reconstructed profile using

$$G_{int}(x) = \int_0^x \Delta G(y) dy = - \int_0^{\frac{2x}{Z_0}} \frac{2}{Z_0} \tilde{P}(\tau) d\tau \quad (16)$$

so that the normalized root-mean-square deviation (NRMSD) error can be written as

$$\epsilon = \frac{\sqrt{\frac{1}{n} \sum_{i=1}^n |\hat{G}_{int}(i) - G_{int}(i)|^2}}{\max\{G_{int}\} - \min\{G_{int}\}}, \quad (17)$$

where  $\hat{G}_{int}(x)$  is a reference value (the simulation result of  $f_c = 50$  GHz and is very close to the exact profile) and  $G_{int}(x)$  is the reconstructed value. In each set-up, the reconstruction error is calculated as the mean of  $\epsilon$  of all trials.

As a baseline comparison we include results from a conventional zero-padding approach. For example, if  $S_{11}$  for  $f_c = 0.5$  GHz is used in Eq. (14) for super-resolution, then the same  $S_{11}$  is zero-padded to  $f_c = 50$  GHz for Eq. (3).

The first set of results are shown in Fig. 4 where  $N_s = 4$ . As is shown in the Fig. 4 (a) where  $f_c = 0.5$  GHz, super-resolution still makes it possible to identify the shunt conductance faults with low error rate (NRMSD).

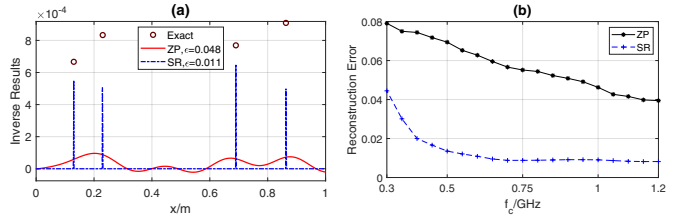


**Fig. 4.** Reconstruction where  $N_s = 4$ . "ZP" is zero-padding and "SR" is super-resolution. (a) An example of the reconstruction where  $f_c = 0.5$  GHz and (b) Reconstruction error with respect to  $f_c$  when there is no noise.

Simulation results for  $N_s = \{7, 6, 5, 4\}$  are shown in Fig. 5 (a). Even with  $f_c$  close to the Rayleigh limit ( $f_c > 0.5$  GHz), super-resolution can still reconstruct the shunt profile with low reconstruction error. Error rate also remains low with noise as shown in Fig. 5 (b).

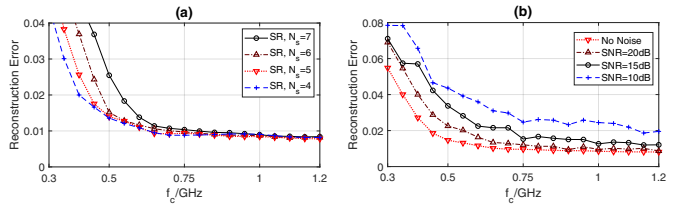


**Fig. 5.** Reconstruction error with respect to  $f_c$ . (a)  $N_s = \{7, 6, 5, 4\}$  with no noise and (b)  $N_s = 5$  for various SNR levels.

#### 5. CONCLUSIONS

We show that super-resolution can be used to precisely locate faults when only limited bandwidth is available. Simulations demonstrate the validity of the approach even when noise is included.

## 6. REFERENCES

- [1] Michael K Ng and Nirmal K Bose, "Mathematical analysis of super-resolution methodology," *IEEE Signal Processing Magazine*, vol. 20, no. 3, pp. 62–74, 2003.
- [2] Emmanuel J Candès and Carlos Fernandez-Granda, "Towards a mathematical theory of super-resolution," *Communications on Pure and Applied Mathematics*, vol. 67, no. 6, pp. 906–956, 2014.
- [3] Leslie Ying and Yi Ming Zou, "Linear transformations and restricted isometry property," in *Acoustics, Speech and Signal Processing, 2009. ICASSP 2009. IEEE International Conference on*. IEEE, 2009, pp. 2961–2964.
- [4] Hayit Greenspan, "Super-resolution in medical imaging," *The Computer Journal*, vol. 52, no. 1, pp. 43–63, 2008.
- [5] Laurent Demanet and Nam Nguyen, "The recoverability limit for superresolution via sparsity," *arXiv preprint arXiv:1502.01385*, 2015.
- [6] Emmanuel J Candès, Justin Romberg, and Terence Tao, "Robust uncertainty principles: Exact signal reconstruction from highly incomplete frequency information," *IEEE Transactions on information theory*, vol. 52, no. 2, pp. 489–509, 2006.
- [7] Q. Zhang, M. Sorine, and M. Admane, "Inverse scattering for soft fault diagnosis in electric transmission lines," *IEEE Transactions on Antennas and Propagation*, vol. 59, no. 1, pp. 141–148, January 2011.
- [8] C. Furse, You Chung Chung, R. Dangol, M. Nielsen, G. Mabey, and R. Woodward, "Frequency-domain reflectometry for on-board testing of aging aircraft wiring," *IEEE Transactions on Electromagnetic Compatibility*, vol. 45, no. 2, pp. 306–315, May 2003.
- [9] Y. J. Shin, E. J. Powers, T. S. Choe, Chan-Young Hong, Eun-Seok Song, Jong-Gwan Yook, and Jin Bae Park, "Application of time-frequency domain reflectometry for detection and localization of a fault on a coaxial cable," *IEEE Transactions on Instrumentation and Measurement*, vol. 54, no. 6, pp. 2493–2500, December 2005.
- [10] M. K. Smail, T. Hacib, L. Pichon, and F. Loete, "Detection and location of defects in wiring networks using time-domain reflectometry and neural networks," *IEEE Transactions on Magnetics*, vol. 47, no. 5, pp. 1502–1505, May 2011.
- [11] F. Loete, Q. Zhang, and M. Sorine, "Experimental validation of the inverse scattering method for distributed characteristic impedance estimation," *IEEE Transactions on Antennas and Propagation*, vol. 63, no. 6, pp. 2532–2538, June 2015.
- [12] Wenjie Wang, Liwen Jing, Zhao Li, and Ross Murch, "Utilizing the Born and Rytov inverse scattering approximations for detecting soft faults in lossless transmission lines," *IEEE Transactions on Antennas and Propagation*, vol. 65, no. 12, pp. 7233–7243, December 2017.
- [13] Liwen Jing, Wenjie Wang, Zhao Li, and Ross Murch, "Detecting impedance and shunt conductance faults in lossy transmission lines," *IEEE Transactions on Antennas and Propagation*, 2018.
- [14] Liwen Jing, Zhao Li, Wenjie Wang, Amartansh Dubey, Pedro Lee, Silvia Meniconi, Bruno Brunone, and Ross D Murch, "An approximate inverse scattering technique for reconstructing blockage profiles in water pipelines using acoustic transients," *The Journal of the Acoustical Society of America*, vol. 143, no. 5, pp. EL322–EL327, 2018.
- [15] Andrew F Colombo, Pedro Lee, and Bryan W Karney, "A selective literature review of transient-based leak detection methods," *Journal of hydro-environment research*, vol. 2, no. 4, pp. 212–227, 2009.
- [16] P. Stoica and A. Nehorai, "Music, maximum likelihood, and cramer-rao bound," *IEEE Transactions on Acoustics, Speech, and Signal Processing*, vol. 37, no. 5, pp. 720–741, May 1989.
- [17] Emmanuel J Candès and Terence Tao, "Decoding by linear programming," *IEEE transactions on information theory*, vol. 51, no. 12, pp. 4203–4215, 2005.
- [18] Marco F Duarte and Yonina C Eldar, "Structured compressed sensing: From theory to applications," *IEEE Transactions on Signal Processing*, vol. 59, no. 9, pp. 4053–4085, 2011.
- [19] Michael Grant and Stephen Boyd, "CVX: Matlab software for disciplined convex programming, version 2.1," <http://cvxr.com/cvx>, Mar. 2014.
- [20] Michael Grant and Stephen Boyd, "Graph implementations for nonsmooth convex programs," in *Recent Advances in Learning and Control*, V. Blondel, S. Boyd, and H. Kimura, Eds., Lecture Notes in Control and Information Sciences, pp. 95–110. Springer-Verlag Limited, 2008, [http://stanford.edu/~boyd/graph\\_dcp.html](http://stanford.edu/~boyd/graph_dcp.html).